

See discussions, stats, and author profiles for this publication at: <https://www.researchgate.net/publication/221879554>

# Nanospecific Inhibition of Pyoverdine Siderophore Production in *Pseudomonas chlororaphis* O6 by CuO Nanoparticles

ARTICLE in CHEMICAL RESEARCH IN TOXICOLOGY · MARCH 2012

Impact Factor: 3.53 · DOI: 10.1021/tx3000285 · Source: PubMed

CITATIONS

22

READS

32

7 AUTHORS, INCLUDING:



**Christian Dimkpa**

International Fertilizer Development Center (I...)

43 PUBLICATIONS 960 CITATIONS

SEE PROFILE



**David W Britt**

Utah State University

63 PUBLICATIONS 1,394 CITATIONS

SEE PROFILE



**William Paul Johnson**

University of Utah

121 PUBLICATIONS 2,817 CITATIONS

SEE PROFILE



**Anne Anderson**

Utah State University

178 PUBLICATIONS 4,726 CITATIONS

SEE PROFILE

# Nanospecific Inhibition of Pyoverdine Siderophore Production in *Pseudomonas chlororaphis* O6 by CuO Nanoparticles

Christian O. Dimkpa,<sup>\*,†,⊥</sup> Joan E. McLean,<sup>‡</sup> David W. Britt,<sup>†</sup> William P. Johnson,<sup>§</sup> Bruce Arey,<sup>||</sup> A. Scott Lea,<sup>||</sup> and Anne J. Anderson<sup>†,⊥</sup>

<sup>†</sup>Department of Biological Engineering, Utah State University, Logan Utah 84322, United States

<sup>‡</sup>Utah Water Research Laboratory, Utah State University, Logan, Utah 84322, United States

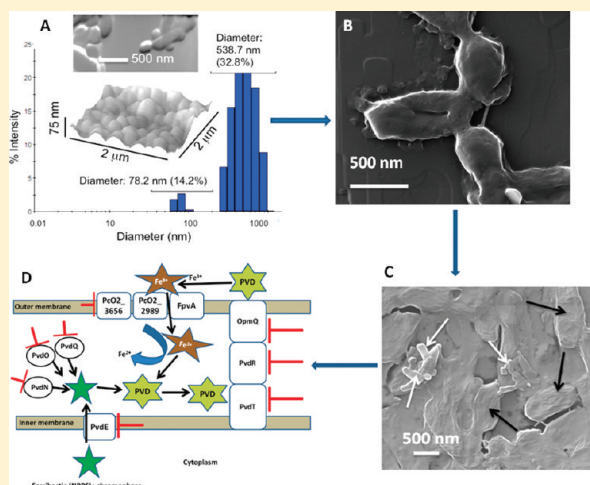
<sup>§</sup>Geology and Geophysics, University of Utah, Salt Lake City, Utah 84112, United States

<sup>||</sup>Pacific Northwest National Laboratory, Richland, Washington 99352, United States

<sup>⊥</sup>Department of Biology, Utah State University, Logan Utah 84322, United States

## Supporting Information

**ABSTRACT:** CuO nanoparticles (NPs) exhibit dose-dependent toxicity to bacteria, whereas sublethal concentrations of these NPs change bacterial metabolism. Siderophores are model metabolites to study the impact of sublethal levels of metallic NPs on bacteria because they are involved in survival and interaction with other organisms and with metals. We report that a sublethal level of CuO NPs modify the production of the fluorescent siderophore pyoverdine (PVD) in a soil beneficial bacterium, *Pseudomonas chlororaphis* O6. The production of PVD was inhibited by CuO NPs but not by bulk CuO nor Cu ions at concentrations equivalent to those released from the NPs. The cell responses occurred despite the NPs forming near micrometer-sized aggregates. The CuO NPs reduced levels of periplasmic and secreted PVD and impaired expression from genes encoding proteins involved in PVD maturation in the periplasm and export through cell membranes. EDTA restored the fluorescence of PVD quenched by Cu ions but did not generate fluorescence with cultures of NP-challenged cells, confirming the absence of PVD. Consequently, depending on the bacterium, this nanoparticle-specific phenomenon mediating cellular reprogramming through effects on secondary metabolism could have an impact on critical environmental processes including bacterial pathogenicity.



## INTRODUCTION

The nanoindustry is projected to be worth US \$1 trillion by 2015.<sup>1</sup> Engineered nanoparticles (NPs) are present in construction materials, paints, antimicrobial coatings, cosmetics, textiles, and recreational equipment.<sup>2</sup> Applications in medicine, pharmaceuticals, catalysis, and electronics are growing exponentially.<sup>3,4</sup> With such diverse uses, NPs inevitably will accumulate in effluents and agricultural settings. Despite the risks, the development of nanoproducts outpaces studies of their interactions with microbes, plants, and humans.<sup>4–6</sup> Depletion of populations of soil microbes through inadvertent exposure to antimicrobial levels of NPs could impair bacterially mediated element cycling, bioremediation, plant growth promotion, and plant stress protection.

Lethality to pathogenic and beneficial bacteria is reported for CuO NPs in part due to the release of Cu ions from the NPs.<sup>7–9</sup> However, few studies<sup>10,11</sup> have investigated the impact of sublethal levels on secondary metabolism that drives bacterial fitness, survival, and benefit to the environment.

Iron is essential for bacteria metabolism but often is scarce due to insolubility at neutral to alkaline pH.<sup>12–17</sup> To overcome this deficiency, most bacteria secrete siderophores to scavenge iron.<sup>12,15,18</sup> Thus, bacteria producing effective siderophores survive better in an Fe-deficient environment, where they antagonize the growth of other microbes through iron deprivation, promote plant growth through iron supply, and regulate toxic metal accumulation in bacteria and plants.<sup>14,16,18–23</sup> Siderophores are employed as a virulence factor in human pathogenic strains such as *Pseudomonas aeruginosa*.<sup>13</sup> Siderophores are, thus, factors significant for maintaining the habitats for most bacteria.

The root-colonizer, *Pseudomonas chlororaphis* O6 (PcO6), increases plant resilience to biotic and abiotic stresses<sup>24,25</sup> and produces the fluorescent siderophore, pyoverdine (PVD),<sup>10</sup> typical for fluorescent pseudomonads.<sup>26,27</sup> Because of their

Received: January 18, 2012

Published: March 1, 2012



importance in bacterial survival and interaction with metals, siderophores are model metabolites to study the impact of sublethal levels of potentially toxic NPs on bacterial cells.

PcO6 shows dose-dependent toxicity with CuO NPs,<sup>9</sup> but at sublethal amounts, PVD levels are reduced. In contrast, ZnO NPs increase PVD levels.<sup>10</sup> Neither CuO nor ZnO NPs alter expression of a gene involved in the biosynthesis of the PVD precursor peptide, ferribactin. However, CuO NPs, but not ZnO NPs, impair expression from *pvdE*,<sup>10</sup> encoding a transporter responsible for exporting ferribactin from the cytoplasm into the periplasm in *P. aeruginosa*.<sup>28,29</sup> These findings suggest that impaired transport from the inner membrane is one facet of the mode of action of CuO NPs. However, maturation of ferribactin to a detectible, fluorescent PVD occurs in the periplasm through several stages. The mature PVD is secreted through the outer membrane by a complex of membrane spanning proteins.<sup>28,29</sup> When loaded with ferric ion from the environment, the PVD-Fe complex passes through specific receptor channels in the outer membrane to be unloaded in the periplasm.<sup>28,30,31</sup> Thus, transcription of an array of specific genes is required for siderophore production and function for iron acquisition by the bacterium.

To better understand the nature of the inhibition of PVD production by CuO NPs, we investigated the effects of a nonlethal amount of CuO NPs on the expression of key PVD-related genes encoding the alternative sigma factor, PvdS, regulating PVD synthesis; proteins involved in the formation of the chromophore portion of the precursor peptide; maturation of ferribactin into PVD in the periplasm; export of mature PVD from the periplasm; and reception of the Fe-loaded PVD at the outer membrane for re-entry into the cell. The responses to the CuO NPs were compared to bulk CuO and to concentrations of Cu ions equivalent to those released from the NPs, allowing us to conclude that the biological effects were nanoparticle-specific. Because Fe inhibits siderophore production, the CuO NPs were characterized for Fe impurity and were sized by dynamic light scattering (DLS) and by atomic force microscopy (AFM). NP surface charge was studied by measuring zeta potential. Interaction of the CuO NPs with the surface of the bacterial cell was imaged by helium ion microscopy (HIM).

## MATERIALS AND METHODS

**Source of Chemicals.** The CuO NPs, Cu ions ( $\text{CuCl}_2$ ), and bulk CuO used in the study were obtained from Sigma Chemical Company (MO, USA). According to manufacturer-provided information, the NPs are <50 nm in size, while the bulk CuO particles are 8000–9000 nm. Inductively Coupled Plasma Mass Spectrometry (ICP-MS) analysis of the CuO NPs in the siderophore-inducing medium (SIM) at pH 6.8<sup>10</sup> was performed to determine the level of Fe present as an impurity, in order to ensure that any effects on PVD production by the NPs will not result from Fe impurity.

**Characterization of CuO NPs in SIM.** Size distribution of the CuO NPs (200 mg/L) in the cell-free medium used to support induction of PVD was analyzed by DLS using a DynaPro NanoStar (Wyatt Technology Corporation, Santa Barbara, CA), with a 658 nm laser. Measurements were made in disposable 50- $\mu\text{L}$  cuvettes (Eppendorf, Germany) and reflect the average of ten five-second acquisitions. The intensity autocorrelation function was converted to a hydrodynamic radius based on the Stokes–Einstein equation using a regularization method employed in the Dynamics software (version 7.0.3, Wyatt Technology Corporation, Santa Barbara, CA). Three separately prepared suspensions of the NPs in growth medium were analyzed.

Tapping mode AFM analysis of suspensions of the CuO NPs deposited from the culture medium on freshly cleaved mica and silicon-oxide surfaces was performed with a Digital Instruments Bioscope NSIIIa using BS-Tap 300 cantilevers as described previously.<sup>32</sup> HIM was performed to image cells and their interaction with CuO NPs (200 mg/L) in SIM. For this, aliquots (10  $\mu\text{L}$ ) of 48 h cultures grown with and without CuO NPs were dried on silicon wafers with a 100 nm oxide layer. The model of HIM was a Carl Zeiss Orion Plus (Peabody, MA, USA) operating at an accelerating voltage of 30 kV and a beam current of approximately 3.0 Pa. Zeta potential measurements to determine NP surface charge, as well as measurement of soluble Cu released from the NPs in the cell-free medium, were performed as previously described.<sup>9</sup>

**Bacterial Strain and Growth Conditions.** The SIM used for cell growth and PVD production was described previously.<sup>10</sup> Control cultures had no amendments. SIM was amended with 200 mg Cu/L CuO NPs chosen because it was sublethal to PcO6.<sup>9,10</sup> To control for particle size, a bulk CuO (200 mg Cu/L) amendment was used as another treatment. The ion levels used were based on the measured solubility from CuO NPs suspended in SIM. The doses were 2 mg Cu/L to mimic release for 1 h, while a second culture was treated at 6 h intervals with installments of Cu ions over 48 h to achieve a final concentration of 21 mg/L, equivalent to the Cu released from the NPs in SIM by 48 h. SIM supplemented with 100  $\mu\text{M}$  Fe ( $\approx 27$  mg/L) from  $\text{FeCl}_3 \cdot 6\text{H}_2\text{O}$  was used as a treatment to inhibit PVD production. Cell growth in the cultures was determined by dilution plating and colony counts.

**Determination of Fluorescent PVD Secretion in PcO6.** Aliquots of 48 h cell cultures with and without amendments of Fe, CuO NPs, Cu ions, or bulk CuO were collected 48 h. The cultures were centrifuged and the supernatants filtered through 0.2  $\mu\text{m}$  filters. The cell-free supernatants from two different growth studies were diluted 1000-fold, and fluorescence of the samples (200  $\mu\text{L}$ ) were read at 398 nm excitation and 460 nm emission<sup>10</sup> using a Synergy4 Hybrid Multi-Mode Micro plate Reader (BioTek, Inc., VT., USA).

**Evaluation of Quenching of PVD Fluorescence by Cu Products.** Cultures were grown for 48 h with and without amendments of 200 mg/L CuO NPs or a total of 21 mg/L Cu ions added stepwise at 6 h intervals. The cells were removed by filtration through 0.2  $\mu\text{m}$  filters. Aliquots of each preparation were amended with EDTA at a final concentration of 0.2 mM ( $\approx 58.5$  mg/L). This concentration was found to restore PVD fluorescence quenched by Cu ions.<sup>32</sup> Fluorescence was determined after incubation for 14 h at 22  $^\circ\text{C}$ .

**Detection of Transcripts from Genes Involved in PVD Production and Export.** Stationary phase cells at 48 h were used as the source of the RNA to evaluate transcript abundance from genes encoding proteins involved in PVD biosynthesis and uptake. The predicted functions of the gene products are described in Supporting Information, section S1. For RNA extraction, cell cultures were pelleted by centrifugation and diluted to an  $\text{OD}_{600\text{ nm}} = 1.0$  to provide equal cell density, and cells from 1 mL were used. RNA extraction was performed using Tri Reagent as described by the manufacturer (Molecular Research Center Inc., OH, USA). DNase treatment of RNA and first-strand cDNA synthesis were performed with the total RNA using a commercially available kit (Fermentas Life Sciences, EU). The elimination of DNA was checked by using the preparation as a template for PCR with primers from the respective genes. RNA and cDNA concentrations were determined with a NanoDrop 2000c spectrophotometer (Thermo Scientific, DE, USA). The gene specific primers used for standard polymerase chain reaction (PCR) amplification and the expected sizes of the respective PCR products are listed in Supporting Information, section S2. The specificity of each primer was verified by their use in PCR with genomic DNA from PcO6 and sequencing the products to confirm the identity of the genes being studied. In control studies, we established the PCR cycle number that would reflect product for each primer set at levels lower than saturation. The final conditions used for the PCR amplification were as follows: initial denaturation at 94  $^\circ\text{C}$  for 2 min, 35 cycles of denaturation at 94  $^\circ\text{C}$  for 30 s, annealing at 62  $^\circ\text{C}$  (except for

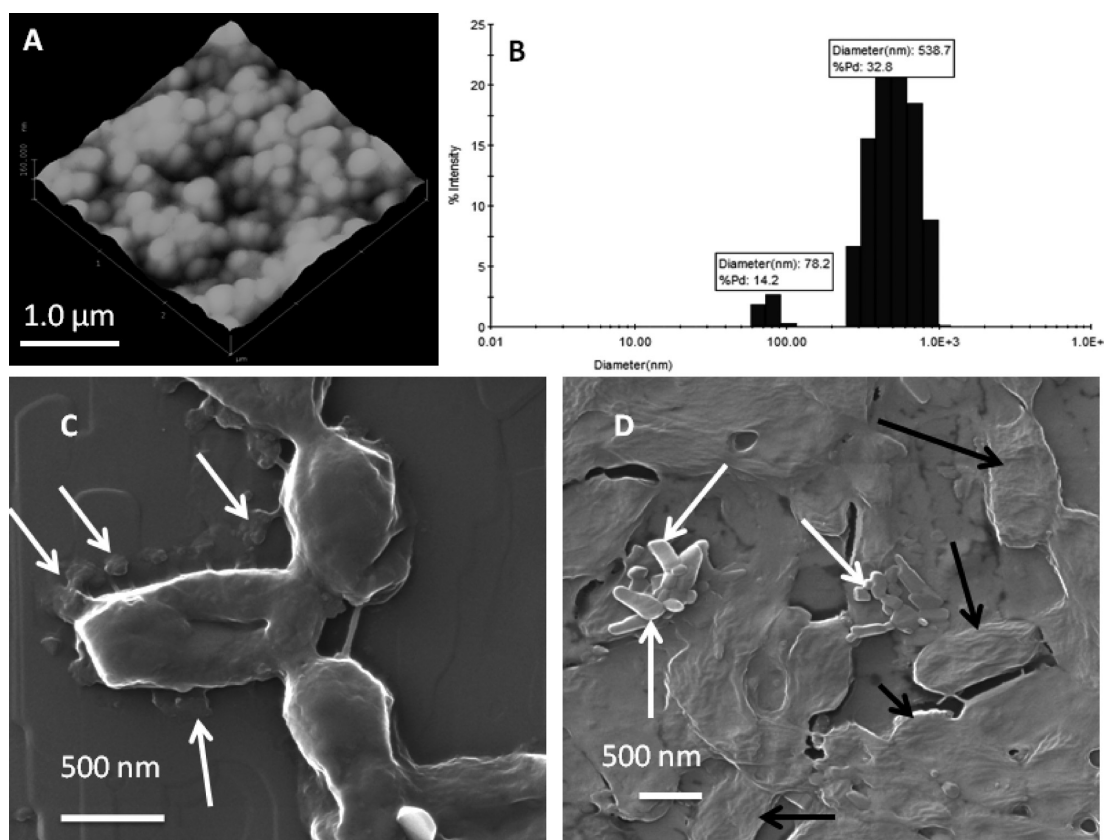


**Figure 1.** CuO NP characterization and imaging of NP–bacterial interactions. (A) Atomic force microscopy image and (B) dynamic light scattering analysis of CuO NP size distribution in the siderophore-inducing medium (SIM). (C) Helium ion microscopy of control *PcO6* cells cultured in SIM revealing cells surfaces showing release of materials resembling outer membrane vesicles (arrows). (D) *PcO6* cells (black arrows) cultured with CuO NPs in SIM are largely obscured by extracellular polymeric substances (EPS), and the NPs (white arrows) are observed as surface clusters in contact with EPS and cells surfaces.

PcO2\_4340, which was annealed at 61 °C) for 30 s, and extension at 72 °C for 40 s. Final extension was performed at 72 °C for 10 min. For PcO2\_4246 and PcO2\_2989, the products (1 mL) from the initial PCR reaction were reamplified because the product levels were low; the second amplification confirmed their production. To control for the RNA levels, PCR products were generated from the 16S rRNA genes using as forward primer GACCGACTACCTGCTCAACG and as reverse primer GGCCAGTGGCAGTTCATATT. PCR amplifications were replicated at least twice, with cells from two independent growth studies.

#### Detection of Periplasmic PVD and the Influence of CuO NPs.

Cells were grown with and without CuO NPs (200 mg Cu/L), 2 mg/L Cu ions, or 100 μM Fe (16.2 mg/L) from FeCl<sub>3</sub>. Cells were harvested by centrifugation after 24, 48, and 72 h and adjusted to an OD<sub>600 nm</sub> = 1.0. Cells were centrifuged and washed twice with water to remove secreted PVD. The periplasmic fractions containing mature and therefore fluorescing PVD were prepared according to the methods described by Katsuwon and Anderson.<sup>34</sup> This method separated the periplasmic and cytoplasmic fractions: any contamination from cytoplasmic ferripectin would not be fluorescent.<sup>29</sup> The fluorescence of the periplasmic fractions was measured as described above.

## RESULTS AND DISCUSSION

**Characterization of CuO NPs.** AFM images of the NPs (Figure 1A) revealed assemblies of particles with less than 75 nm height and lateral dimensions between 100 and 1000 nm. DLS analysis supported AFM imaging, showing two particle size fractions of the CuO NPs when suspended in SIM. There was a 78 nm size fraction, larger than the <50 nm size provided by the manufacturer, but most of the mass aggregated into

submicrometer sized particles with a mean diameter of 539 nm (Figure 1B). HIM of unchallenged *PcO6* cells (Figure 1C) showed individual cells connected by threads of extracellular polymeric substances. Structures resembling vesicles blebbing from the cell surface were apparent. Growth of *PcO6* with CuO NPs caused the cell shape to be obscured by coatings with an extracellular layer (Figure 1D). HIM revealed individual and aggregates of CuO NPs bound to this layer and exhibiting a range of sizes and geometries in agreement with the AFM and DLS data. Association between NPs and the bacterial cell surface could be initiated through charge interactions. We found that visible NP colloids in SIM had a mean zeta potential of ≈38.0 mV; these positively charged particles would readily bind to the negatively charged cell surface.<sup>9</sup>

The CuO NPs (200 mg Cu/L) released soluble Cu with incubation in SIM (pH 6.8); soluble Cu was  $2 \pm 0.05$ ,  $14 \pm 0.5$ , and  $21 \pm 7.4$  μg/L at 1, 24, and 48 h, respectively. Analysis of the CuO NPs by ICP-MS, to determine that they did not contribute Fe to the medium that would influence PVD production, revealed 11.8 μg/L (≈ 0.04 μM) Fe to be present in the 200 mg Cu/L CuO NP preparation. This level was below the 1 μM level reported to prevent siderophore production in microbes.<sup>12</sup> We show that with *PcO6*, Fe amendments to SIM in the range of 0–0.1 mg/L did not prevent siderophore production (Supporting Information, section S3).

**CuO NPs Inhibit PVD Secretion.** Colony counts on dilution plating (cfu/mL) indicated that cell growth to stationary phase at 48 h was not impaired by treatments with



**Table 1. Effects of CuO NPs, Cu Ions, and Bulk CuO on Cell Growth and Fluorescence in the Medium Characteristic of Pyoverdine (PVD) Siderophores<sup>a</sup>**

treatment/response	control	Fe (100 $\mu$ M)	CuO NPs (200 mg/L)	Cu ions (2 mg/L)	Cu ions (21 mg/L)	bulk CuO (200 mg/L)
cell count (log <sub>10</sub> CFU/mL)	12.7 $\pm$ 0.15	12.0 $\pm$ 0.1	12.3 $\pm$ 0.25	12.2 $\pm$ 0.13	12.5 $\pm$ 0.38	12.4 $\pm$ 0.2
extracellular fluorescence (RFU $\times$ 10 <sup>3</sup> )	28,464 $\pm$ 3361 a	276 $\pm$ 20 b	1085 $\pm$ 55 b	29,067 $\pm$ 2759 a	1083 $\pm$ 118 b	32,223 $\pm$ 1802 a

<sup>a</sup>Cell growth was measured by counting cell colonies on dilution plates after 48 h. PVD was measured as relative fluorescence units (RFU) with excitation/emission = 398/460 nm on 1000-fold diluted samples of cell-free supernatants after 48 h of growth in SIM. Two Cu ion treatments were used: a single application of 2 mg/L and a second treatment where ions were added incrementally to total 21 mg/L Cu ion treatment over a 48 h period. Data shown are means and SDs of measurements ( $n = 3$ ) from two different cell growth studies, and for extracellular PVD fluorescence, different letters after values represent significant differences between treatments ( $p = 0.05$ ).

the NPs and bulk CuO. Cu ions provided as a single (2 mg/L) or multiple additions to a final concentration of 21 mg/L also did not affect cell growth (Table 1). These observations agreed with our prior findings.<sup>10,11</sup> We used the fluorescence of the PVD to determine their relative abundance in cell-free growth medium. Fluorimetry confirmed secretion to high levels in unamended cultures and reduced levels upon addition of Fe or CuO NPs (Table 1). Amendments of 2 mg/L Cu ions and bulk CuO (200 mg Cu/L) did not change the PVD level. The use of multiple additions of Cu ions to total 21 mg/L in 48 h-cultures reduced fluorescence to the levels of amendments with Fe and CuO NPs (Table 1). Thus, both Cu ions (at high concentration) and CuO NPs affected the levels of PVD detected by fluorescence in the culture medium. The pHs of the culture supernatants after 48 h were 6.50 (control), 6.26 (CuO NPs), 6.49 (2 mg/L Cu ions), and 6.53 (21 mg/L Cu ions). Therefore, growth of the *PcO6* cells alone as well as the growth in the Cu treatments slightly acidified the medium, with the CuO NPs treatment causing the highest change in pH. These slight changes in pH were unlikely to affect the PVD fluorescence directly to any great extent.<sup>33</sup>

**Cu Ions Quench PVD Fluorescence, Which Is Restored by EDTA.** The low PVD fluorescence in cultures amended with 21 mg/L Cu ions was explained by quenching of fluorescence of PVD by the ions. Data shown in Figure 2 revealed that addition of another chelator, EDTA, to cell-free supernatants of SIM in which *PcO6* had been grown for 48 h with 21 mg/L Cu ions restored PVD fluorescence to the level observed in the control cultures. Geochemical modeling<sup>35</sup> indicated that the EDTA concentration used would chelate 60% of Cu ions, with 19% remaining associated with the PVD. These findings showed that PVD was being produced in the cultures containing Cu ions and that its detection was prevented by quenching as the Cu ions interacted with the siderophore.<sup>10,33</sup> In contrast, fluorescence was not observed when EDTA was added to the culture medium from cells grown for 48 h with CuO NPs amendments (Figure 2). This finding confirmed that the lack of fluorescence characteristic of PVD in the cultures containing CuO NPs was due to its absence, rather than quenching of fluorescence by Cu ions released from the NPs.

**CuO NPs Modify the Expression of PVD-Related Genes in *PcO6*.** To explore the mechanism by which the CuO NPs reduced PVD levels, expression from genes involved in PVD synthesis and function was examined. Many of these genes are clustered on the *PcO6* genome between locus tags 4240 and 4340 (see ref 10 and Supporting Information, section S2). BLASTn analysis showed high identity between the *PcO6* genes and those from *P. aeruginosa* and other pseudomonads (Table S1, Supporting Information), where mutational studies have characterized their functions.<sup>13,27–29,36–40</sup> We used

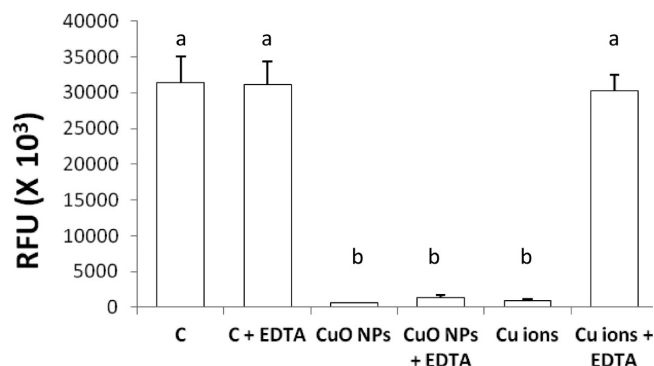


**Figure 2.** Restoration by EDTA of PVD fluorescence quenched by Cu ions compared to the control (C). Cell-free culture media were prepared by filtration from 48 h cultures grown with and without amendments of CuO NPs (200 mg Cu/L) or 21 mg Cu ions. One sample of each culture medium was left unamended, whereas a second sample was mixed with EDTA (0.2 mM final concentration) for 14 h, when fluorescence measurements (excitation/emission = 398/460 nm) were taken on  $\times$ 1000-fold diluted preparations. Data are means and SDs (in some sufficiently low to not be visible) of the measurements ( $n = 3$ ) of two different studies; different letters on bars indicate significant differences among the treatments ( $p = 0.05$ ). RFU = Relative Fluorescence Units.

reverse transcription (RT)-PCR to examine gene expression, normalizing the data with expression from the 16S rRNA genes that was similar for each treatment (Figure 3A, left panel). However, expression from the gene at locus tag *PcO2\_4340*, orthologous to *pvdS* in *P. aeruginosa* PA01 encoding a regulatory sigma factor, was repressed by 100  $\mu$ M Fe compared to the control treatment. In contrast, expression from *PcO2\_4340* was little altered in the cells grown with CuO NPs or Cu ions (Figure 3A, center panel). The gene at locus tag *PcO2\_4339* showed 83% identity to *pvdL* in *P. aeruginosa*, which encodes a protein involved in the nonribosomal synthesis of the chromophore peptide. Although *PcO2\_4340* and *PcO2\_4339* are contiguous, these genes are predicted to be transcribed in opposite directions.<sup>10</sup> Addition of Fe repressed the expression of *pvdL*, as anticipated. Amendment with CuO NPs lowered the transcript level, while 2 mg/L Cu ions had no effect on transcript level compared to control cells (Figure 3A, right panel).

Genes with identity similar to those in *P. aeruginosa* encoding proteins involved in PVD maturation in the periplasm<sup>29</sup> are located at locus tags *PcO2\_4243* (*pvdP*), *PcO2\_4244* (*pvdQ*), *PcO2\_4245* (*pvdN*) and *PcO2\_4246* (*pvdO*). Surprisingly, no transcripts were detected from the *pvdP* ortholog at *PcO2\_4243* in cells grown in SIM, despite 83% with *pvdP* from *P. aeruginosa* (Figure 3B). This gene is transcribed in a

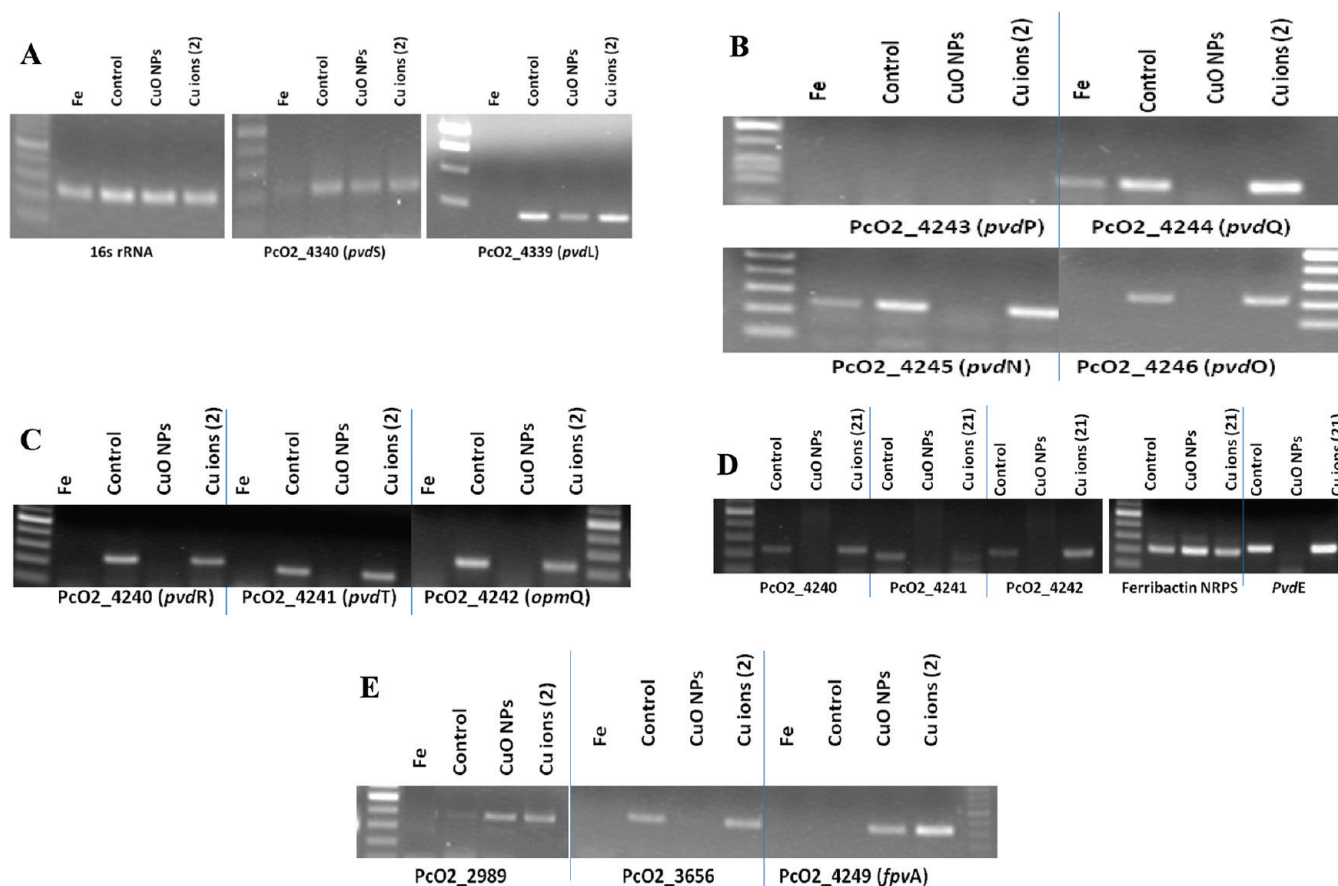


**Figure 3.** Gel electrophoresis images of PCR products from cDNA prepared from RNA extracted from cells cultured with and without Fe (100  $\mu$ M), Cu (2 or 21 mg/L) ions, or CuO NPs (200 mg Cu/L). Transcript abundance was measured for (A) 16 S rRNA genes, used as controls for normalization: PVD chromophore biosynthesis gene (*PcO2\_4339*) and PVD biosynthesis regulatory gene, *pvdS* (*PcO2\_4340*). (B) Genes involved in PVD maturation in the periplasm. (C) Genes mediating export and recycling of PVD at the outer membrane. (D) Effect of an incremental addition of Cu ions, to a final Cu concentration of 21 mg/L in 48 h cultures, on transcript accumulation from genes directing the biosynthesis (NRPS), inner membrane transport into the periplasm (PvdE), and secretion into the environment via the inner membrane-periplasmic-outer membrane efflux channel (*PcO2\_4240-4242*) compared to control (no metal amendment) and CuO NP (200 mg Cu/L)-treated cells. (E) Genes encoding receptors mediating uptake of the PVD-Fe complex. Data are representative of two or more PCR amplifications from RNA from three different growth cultures. DNA molecular weight markers (100 bp) are shown in the first or/and last lane of each image. Images for *PcO2\_4246* (B) and *PcO2\_2989* (E) are derived from a second amplification of the products (1 mL) from the initial PCR reactions.

different direction than *PcO2\_4244-45-46*,<sup>10</sup> it is possible that its gene product is not essential for PVD maturation in *PcO6* under the conditions of our study. In contrast, transcripts were found from genes orthologous to *pvdQ*, *pvdN*, and *pvdO*. As anticipated, Fe reduced the transcript levels from these genes. Expression also was reduced from each gene by growth of cells with CuO NPs but not with Cu ions.

In *P. aeruginosa*, export of newly formed PVD and recycling of PVD released from the Fe-loaded complex imported into the periplasm is mediated by products from *pvdRT-opmQ*,<sup>28,38,39</sup> corresponding in *PcO6* to genes at locus tags *PcO2\_4240*, *PcO2\_4241*, and *PcO2\_4242*. *PvdT* is an inner membrane ATP-binding permease, connected to *PvdR*, a periplasmic adaptor protein that interacts with the outer membrane-bound channel protein, *OpmQ*. In *P. aeruginosa*, these genes form an operon.<sup>28,38,39</sup> In *PcO6*, only 1 bp of DNA separates *pvdR* and *pvdT*, and the space between *pvdT* and *OpmQ* is only 8 bp long, suggesting that these genes too are within an operon. A conserved iron-starvation (IS) consensus box, TAAAT, characterizing *PvdS*-regulated genes,<sup>40,41</sup> was present upstream of *PcO2\_4242*. Expression from this operon was repressed by Fe and the CuO NPs, in comparison to transcript accumulation

in control and Cu ion (2 mg Cu/L)-treated cells (Figure 2C). Treatment of the cells treated with 21 mg Cu ion/L also did not repress expression of this gene (Figure 3D, left panel). We confirmed our earlier findings<sup>10</sup> that CuO NPs did not repress transcripts from the gene at locus tag *PcO2\_6540* (formerly 4251) involved in the synthesis of ferribactin but repression of *pvdE*, encoding the inner membrane transporter for ferribactin. On the basis of the band intensities, transcript accumulation from genes involved with synthesis of ferribactin NRPS was unaffected, while that from *pvdE* was slightly stimulated by Cu ions at a high dose (21 mg Cu/L) compared to control (Figure 3D, right panel).

Uptake of Fe-loaded PVD from the environment into the cell is achieved by different outer-membrane-bound receptors in *P. aeruginosa*, mainly *FpvA*, and to a lesser degree *FpvB*.<sup>30,31,42</sup> Studies of the effect of CuO NPs on the expression of genes encoding potential PVD-Fe receptors at the locus tags *PcO2\_2989*, *PcO2\_3656*, and the *fpvA*-orthologue *PcO2\_4249* (Supporting Information, section S1) showed different regulations. Fe repressed expression from all three genes. Weak expression was noted from loci *PcO2\_2989* and no expression from *PcO2\_4249* in control cells lacking Cu

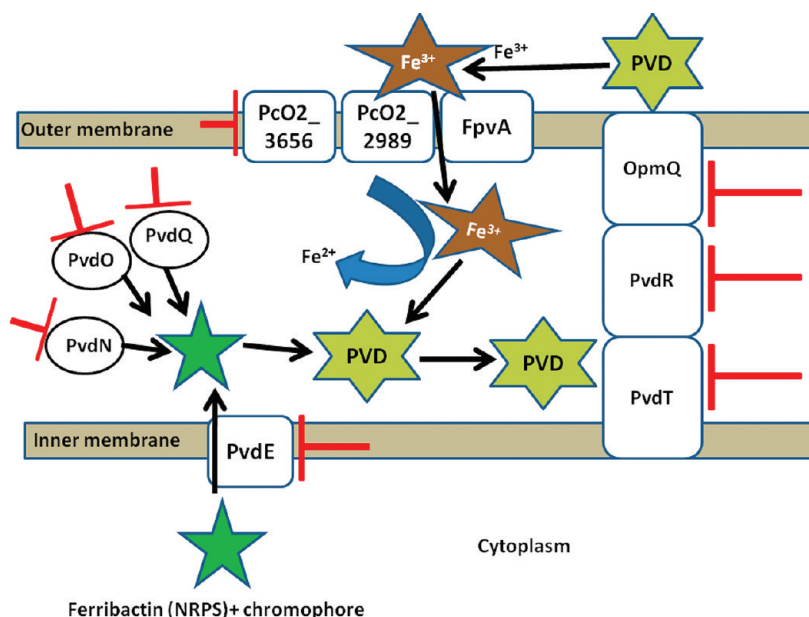


**Figure 4.** Schematic representation of steps where CuO NPs impaired the production of proteins involved in PVD transport and maturation in *PcO6*. The proteins targets shown by the red blocks are predicted based on evidence from RT-PCR analysis of reduced expression from the gene encoding the proteins in cells exposed to CuO NPs. These changes would account for the low periplasmic and external PVD levels observed with *PcO6* cells contacted by the CuO NPs. Ferric ion is scavenged in the environment by secreted PVD, and the complex is received at the outer membrane by one or more of the receptors and internalized. The ferric ion is reduced to ferrous ion in the periplasm<sup>28</sup> and used for metabolism. The free PVD is recycled to the cell exterior via the PvdRT-OpmQ efflux pump. Efflux of newly synthesized PVD also involves this channel.

challenge (Figure 3E). Expression from PcO2\_2989 and PcO2\_4249 was enhanced by both CuO NPs and 2 mg/L Cu ions. Expression from PcO2\_3656 showed the same pattern of regulation as the genes for PVD maturation and those in the operon for PVD export: induction in the control cells and cells exposed to Cu ion, and repression in cells grown with CuO NPs (Figure 3E). These findings suggest that PcO2\_2989 and to a greater extent PcO2\_3656, but not PcO2\_4249, are the default genes for PVD-Fe uptake in *PcO6*. In *P. aeruginosa*, FpvA binds Al-loaded PVD and permit uptake of the metal into the cell, whereas Al-free PVD show little or no affinity to this receptor.<sup>30</sup> Siderophores bind Cu ions, though with reduced affinity compared with Fe ions.<sup>19,43</sup> Thus, the induction of the receptors PcO2\_3656 and PcO2\_4249 by Cu-challenge in *PcO6* demonstrates that they potentially could permit PVD-Cu ion uptake. Collectively, these studies on gene expression indicate that the CuO NPs repressed expression of genes involved in transport to and maturation of PVD in the periplasm, its export through the outer membrane, and import of the loaded PVD. Because these changes were not duplicated by low (2 mg Cu/L) or high (21 mg Cu/L) levels of Cu ions, the effects were NP specific. We summarize the effects of the CuO NPs on PVD formation and function in *PcO6* in Figure 4, showing a major impact was impaired expression of specific genes. These effects are not generalized to other metal oxide NPs nor to other bacterial secondary metabolites; as reported earlier, challenge with ZnO NP stimulated PVD production by mechanisms that in part correlated with release of Zn ions from the NPs.<sup>10</sup> In contrast to PVD, these same CuO NPs promoted in *PcO6* the production of IAA, a plant-growth promoting secondary compound.<sup>11</sup>

Ingress of NPs to the bacterial cytoplasm has been reported for other metallic NPs,<sup>44,45</sup> and a nanoparticle effect on gene expression was suggested for the genotoxicity of silver and CuO NPs in *E. coli* and plants, respectively.<sup>46,47</sup> Similarly, CuO NPs

damaged DNA in human lung epithelial cells and were more cytotoxic than Cu ions.<sup>48</sup> In these studies with *PcO6*, we have observed NP-specific effects on secondary metabolism related to altered gene expression. It is interesting that Hofte et al.<sup>49</sup> reported that a site-specific recombinase regulated PVD synthesis independently of PvdS in *P. aeruginosa*. Because the recombinases are associated with DNA rearrangements, we speculate that the CuO NPs may incite changes to the DNA.

**CuO NPs Reduce PVD Levels in the Periplasm.** The findings that CuO NPs reduced transcription from genes involved in PVD transport and maturation and the demonstration of the reduced PVD secretion out of the cell suggested the CuO NPs would alter the levels of PVD observed in the periplasm. We confirmed this possibility by measuring fluorescent PVD levels in the periplasm. Periplasmic extracts from *PcO6* cells grown in SIM without amendments for 24, 48, and 72 h displayed fluorescence (Figure 5). Fluorescence was reduced significantly ( $p = 0.05$ ) by inclusion of Fe in the culture medium, as anticipated from inhibited gene expression. Amendment of cultures with 2 mg/L Cu ions for 24 and 48 h increased fluorescence significantly from the control cultures. However, the periplasmic extracts of CuO NP-grown cells had fluorescence below that of the control cells (Figure 5). This finding was consistent with reduced transport of product into the periplasm and maturation in that cell compartment, as expected from impaired expression from the *pvdE* transport<sup>10</sup> and the periplasmic maturation genes.

Changes in gene expression and production of fluorescent PVD were induced by the CuO NPs although our characterization showed that the particles existed largely in an aggregate state. However, inhibition of PVD production did not occur with bulk CuO, nor with exposure to Cu ions at concentrations equivalent to their release from the NPs. Thus, the observed reduction in PVD production from the beneficial soil microbe, *PcO6*, was a nanospecific effect. HIM showed physical



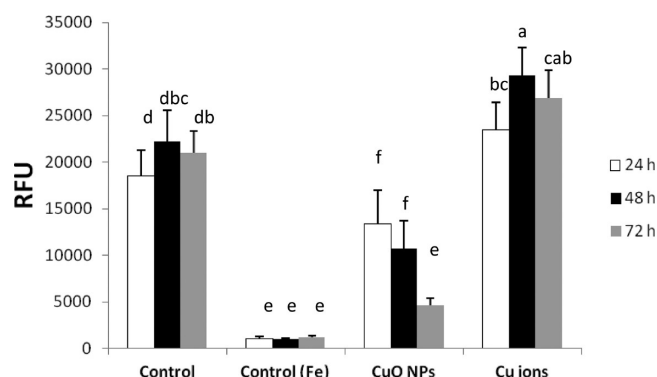


**Figure 5.** Relative Fluorescence Units (RFU) of PVD in periplasmic fractions of *PcO6* cells grown in the absence or presence of ferric ion (100  $\mu$ M), CuO NPs (200 mg Cu/L), and Cu ions (2 mg Cu/L). Fluorescence measurements (excitation/emission = 398/460 nm) were taken with undiluted periplasmic fractions prepared from 24, 48, and to 72 h cultures. Data are the means and SDs of the measurements ( $n = 3$ ) of two different studies, and different letters on bars indicate significant differences among the treatments at all time points ( $p = 0.05$ ).

association of CuO NPs with the bacterial cell surface that appeared to be modified by production of extracellular materials obscuring cell outlines. This observation suggested that other changes in bacterial metabolism occurred in addition to the impact of the NPs on PVD production. Previously, we reported that the extracellular matrix materials from planktonic *PcO6* cells alleviated loss in culturability upon exposure to Ag and CuO NPs, as well as Ag and Cu ions.<sup>9,32</sup> Stimulation of extracellular matrix production by ZnO NPs also occurred with *Escherichia coli* and *Shewanella oneidensis*.<sup>50</sup>

Under our test conditions, we did not observe changes in gene expression of most of our target genes by Cu ions, although others have reported such changes from activation to inhibition for genes related to siderophore production.<sup>36,51</sup> Previously, we showed Cu ions bound to pseudomonad cells<sup>52</sup> and were compartmentalized in the periplasm and the cytoplasm changing expression of genes involved in cell protection.<sup>53</sup> Cell death occurred with *PcO6* at 2.5 mg/L ions, and we implicated released of ions from CuO NPs being involved in toxicity because cells were protected from killing by the presence of a Cu ion-specific chelator, bathocuproine.<sup>9</sup> Our findings demonstrate again that CuO NPs present in the environment as contaminants would act as a point source for Cu ion release. Ion release from NPs and their reduction by environmental factors has been implicated in remodeling of NP size and shape in studies for Cu and Ag NPs.<sup>54</sup>

## CONCLUSIONS

A sublethal dose of CuO NPs impaired PVD function in a Gram-negative bacterium. Inhibited expression from genes involved in siderophore maturation and transport contributed to reduced siderophore levels in the periplasm and export through the outer membrane of the beneficial soil pseudomonad. By comparison to treatments with Cu ions and bulk CuO, these effects appear to be specific to the CuO NPs. The effects were not related to Fe contaminants in the NP formulation; however, the presence of other unknown contaminants in the NP formulation that may influence siderophore production remains undetermined at this time. Siderophores have commanding roles in the interactions between bacteria and

other microbes, and with plants and humans. Considering the tonnage at which NP-containing materials are produced and used, it is likely that there will be environmental contamination by NPs. We demonstrate in this work that NPs may influence cellular functions with significance more broad than just their killing capacity. At sublethal levels, NPs may provoke bacterial cellular reprogramming with an impact on secondary metabolism with environmental and medical implications.

## ASSOCIATED CONTENT

### Supporting Information

Identities and predicted functions of *Pseudomonas chlororaphis* O6 genes investigated in this study; sequences, melting temperatures of primers used for PCR analysis of PVD genes, and the expected PCR product sizes of the genes; and use of the universal chrome azurol S (CAS) assay to demonstrate the noninhibition of siderophore production by trace levels of Fe above the range present as impurity in commercial CuO NPs. This material is available free of charge via the Internet at <http://pubs.acs.org>.

## AUTHOR INFORMATION

### Corresponding Author

\*Tel: 001-435-7973497. E-mail: [cdimkpa@usu.edu](mailto:cdimkpa@usu.edu).

### Funding

This work was supported by the USDA-CSREES grant 2009-35603-05037, the Utah Agricultural Experiment Station (Journal Paper # 8323), and the Utah Water Research Laboratory.

### Notes

The authors declare no competing financial interest.

## ACKNOWLEDGMENTS

We thank Eliana Manangón for assistance with DLS measurements. Helium ion microscopy was performed using EMSL, a U.S. national scientific user facility sponsored by the Department of Energy's Office of Biological and Environmental Research and located at Pacific Northwest National Laboratory.

## ABBREVIATIONS

AFM, atomic force microscopy; CuO, copper oxide; DLS, dynamic light scattering; Fe, ferric iron; HIM, helium ion microscopy; IAA, indole-3-acetic acid; NP, nanoparticles; CFU, colony forming unit; RT-PCR, reverse transcription polymerase chain reaction; *PcO6*, *Pseudomonas chlororaphis* O6; PVD, pyoverdine; RFU, relative fluorescence unit; SIM, siderophore-inducing medium

## REFERENCES

- (1) Nel, A., Xia, T., Mädler, L., and Li, N. (2006) Toxic potential of materials at the nanolevel. *Science* 311, 622–667.
- (2) Lee, J., Mahendra, S., and Alvarez, P. J. (2010) Nanomaterials in the construction industry: a review of their applications and environmental health and safety considerations. *ACS Nano* 4, 3580–3590.
- (3) Khang, D., Carpenter, J., Chun, Y. W., Pareta, R., and Webster, T. J. (2010) Nanotechnology for regenerative medicine. *Biomed. Microdevices* 12, 575–587.
- (4) Shvedova, A. A., Kagan, V. E., and Fadeel, B. (2010) Close encounters of the small kind: adverse effects of man-made materials interfacing with the nano-cosmos of biological systems. *Annu. Rev. Pharmacol. Toxicol.* 50, 63–88.



- (5) Behra, R., and Krug, H. (2008) Nanoecotoxicology: Nanoparticles at large. *Nature Nanotechnol.* 3, 253–254.
- (6) Rico, C. M., Majumdar, S., Duarte-Gardea, M., Peralta-Videa, J. R., and Gardea-Torresdey, J. L. (2011) Interaction of nanoparticles with edible plants and their possible implications in the food chain. *J. Agric. Food. Chem.* 59, 3485–3498.
- (7) Gunawan, C., Teoh, W. C., Marquis, C. P., and Amal, R. (2011) Cytotoxic origin of copper(II) oxide nanoparticles: comparative studies with micron-sized particles, leachate, and metal salts. *ACS Nano* 5, 7214–7225.
- (8) Gajjar, P., Pettee, B., Britt, D. W., Huang, W., Johnson, W. P., and Anderson, A. J. (2009) Antimicrobial activities of commercial nanoparticles against an environmental soil microbe, *Pseudomonas putida* KT2440. *J. Biol. Eng.* 3, 9.
- (9) Dimkpa, C. O., Calder, A., McLean, J. E., Britt, D. W., and Anderson, A. J. (2011) Responses of a soil bacterium, *Pseudomonas chlororaphis* O6 to commercial metal oxide nanoparticles compared with responses to metal ions. *Environ. Pollut.* 159, 1749–1756.
- (10) Dimkpa, C. O., McLean, J. E., Britt, D. W., and Anderson, A. J. (2011) CuO and ZnO nanoparticles differently affect the secretion of fluorescent siderophores in the beneficial root colonizer *Pseudomonas chlororaphis* O6. *Nanotoxicology*, DOI 10.3109/17435390.2011.598246.
- (11) Dimkpa, C. O., Zeng, J., McLean, J. E., Britt, D. W., Zhan, J., and Anderson, A. J. (2012) Production of indole-3-acetic acid via the indole-3-acetamide pathway in the plant-beneficial bacterium, *Pseudomonas chlororaphis* O6 is inhibited by ZnO nanoparticles but enhanced by CuO nanoparticles. *Appl. Environ. Microbiol.* 78, 1404–1410.
- (12) Neilands, J. B. (1995) Siderophores: structure and function of microbial iron transport compounds. *J. Biol. Chem.* 270, 26723–26726.
- (13) Lamont, I. L., Beare, P. A., Ochsner, U., Vasil, A. I., and Vasil, M. L. (2002) Siderophore-mediated signaling regulates virulence factor production in *Pseudomonas aeruginosa*. *Proc. Natl. Acad. Sci. U.S.A.* 99, 7072–7077.
- (14) Kloepper, J. W., Leong, J., Teintze, M., and Schroth, M. N. (1980) Enhanced plant growth by siderophores produced by plant growth-promoting rhizobacteria. *Nature* 286, 885–886.
- (15) Poole, K., and McKay, G. A. (2003) Iron acquisition and its control in *Pseudomonas aeruginosa*: many roads lead to Rome. *Front. Biosci.* 8, d661–686.
- (16) Haas, D., and Defago, G. (2005) Biological control of soil-borne pathogens by fluorescent pseudomonads. *Nature Rev. Microbiol.* 3, 307–319.
- (17) Sarkar, S. F., Gordon, J. S., Martin, G. B., and Guttman, D. S. (2006) Comparative genomics of host-specific virulence in *Pseudomonas syringae*. *Genetics* 174, 1041–1056.
- (18) Dimkpa, C., Merten, D., Svatoš, A., Büchel, G., and Kothe, E. (2008) Hydroxamate siderophores produced by *Streptomyces acidiscabies* E13 bind nickel and promote growth in cowpea (*Vigna unguiculata* L.) under nickel stress. *Can. J. Microbiol.* 54, 163–172.
- (19) Dimkpa, C. O., Merten, D., Svatoš, A., Büchel, G., and Kothe, E. (2009) Metal-induced oxidative stress impacting plant growth in contaminated soil is alleviated by microbial siderophores. *Soil Biol. Biochem.* 41, 154–162.
- (20) Dimkpa, C., Merten, D., Svatoš, A., Büchel, G., and Kothe, E. (2009) Siderophores mediate reduced and increased uptake of cadmium by *Streptomyces tendae* F4 and sunflower (*Helianthus annuus*), respectively. *J. Appl. Microbiol.* 107, 1687–1696.
- (21) Dimkpa, C. O., Svatoš, A., Dabrowska, P., Schmidt, A., Boland, W., and Kothe, E. (2008) Involvement of siderophores in the reduction of metal-induced inhibition of auxin synthesis in *Streptomyces* spp. *Chemosphere* 74, 19–25.
- (22) Vansuyt, G., Robin, A., Briat, J.-F., Curie, C., and Lemanceau, P. (2007) Iron acquisition from Fe-pyoverdine by *Arabidopsis thaliana*. *Mol. Plant-Microbe Interact.* 20, 441–447.
- (23) Braud, A., Geoffroy, V., Hoegy, F., Mislin, G. L. A., and Schalk, I. J. (2010) Presence of the siderophores pyoverdine and pyochelin in the extracellular medium reduces toxic metal accumulation in *Pseudomonas aeruginosa* and increases bacterial metal tolerance. *Environ. Microbiol. Rep.* 2, 419–425.
- (24) Spencer, M., Kim, Y. C., Ryu, C. M., Kloepper, J., Yang, Y. C., and Anderson, A. J. (2003) Induced defence in tobacco by *Pseudomonas chlororaphis* strain O6 involves at least the ethylene pathway. *Mol. Plant-Microbe Interact.* 63, 27–34.
- (25) Ryu, C. M., Kang, B. R., Han, S. H., Cho, S. M., Kloepper, J. W., Anderson, A. J., and Kim, Y. C. (2007) Tobacco cultivars vary in induction of systemic resistance against Cucumber mosaic virus and growth promotion by *Pseudomonas chlororaphis* O6 and its *gacS* mutant. *Euro. J. Plant Pathol.* 119, 383–390.
- (26) Cornelis, P., and Matthijs, S. (2002) Diversity of siderophore-mediated iron uptake systems in fluorescent pseudomonads: not only pyoverdines. *Environ. Microbiol.* 4, 787–798.
- (27) Braud, A., Hoegy, F., Jezequel, K., Lebeau, T., and Schalk, I. J. (2009) New insights into the metal specificity of the *Pseudomonas aeruginosa* pyoverdine-iron uptake pathway. *Environ. Microbiol.* 11, 1079–1091.
- (28) Imperi, F., Tiburzi, F., and Visca, P. (2009) Molecular basis of pyoverdine siderophore recycling in *Pseudomonas aeruginosa*. *Proc. Natl. Acad. Sci. U.S.A.* 106, 20440–20445.
- (29) Yeterian, E., Martin, L. W., Guillon, L., Journet, L., Lamont, I. L., and Schalk, I. J. (2010b) Synthesis of the siderophore pyoverdine in *Pseudomonas aeruginosa* involves a periplasmic maturation. *Amino Acids* 38, 1447–1459.
- (30) Greenwald, J., Zeder-Lutz, G., Hagege, A., Celia, H., and Pattus, F. (2008) The metal dependence of pyoverdine interactions with its outer membrane receptor FpvA. *J. Bacteriol.* 190, 6548–6558.
- (31) Ghysels, B., Dieu, B. T. M., Beatson, S. A., Pirnay, J.-P., Ochsner, U. A., Vasil, M. L., and Cornelis, P. (2004) FpvB, an alternative type I ferripyoverdine receptor of *Pseudomonas aeruginosa*. *Microbiology* 150, 1671–1680.
- (32) Dimkpa, C. O., Calder, A., Gajjar, P., Merugu, S., Huang, W., Britt, D. W., McLean, J. E., Johnson, W. P., and Anderson, A. J. (2011) Interaction of silver nanoparticles with an environmentally beneficial bacterium *Pseudomonas chlororaphis*. *J. Hazard. Mater.* 188, 428–235.
- (33) Xiao, R., and Kisaalita, W. (1995) Purification of pyoverdines of *Pseudomonas fluorescens* 2–79 by copper-chelate chromatography. *Appl. Environ. Microbiol.* 61, 3769–3774.
- (34) Katsuwon, J., and Anderson, A. J. (1990) Catalase and superoxide dismutase of root-colonizing saprophytic fluorescent pseudomonads. *Appl. Environ. Microbiol.* 56, 3576–3582.
- (35) Parker, D. R., Norvell, W. A., and Chaney, R. L. (1995) GEOCHEM-PC: A Chemical Speciation Program for IBM and Compatible Personal Computers, in *Chemical Equilibrium and Reaction Models* (Loeppert, R. H., Schwab, A. P., and Goldberg, S., Eds.) pp 253–270, Soil Science Society of America, Madison, WI.
- (36) Teitzel, G. M., Geddie, A., De Long, S. K., Kirisits, M. J., Whiteley, M., and Parsek, M. R. (2006) Survival and growth in the presence of elevated copper: Transcriptional profiling of copper-stressed *Pseudomonas aeruginosa*. *J. Bacteriol.* 188, 7242–7256.
- (37) Mossialos, D., Ochsner, U., Bayse, C., Chablain, P., Pirnay, J.-P., Koedam, N., Budzikiewicz, H., Fernandez, D. U., Schafer, M., Ravel, J., and Cornelis, P. (2002) Identification of new, conserved, non-ribosomal peptide synthetases from fluorescent pseudomonads involved in the biosynthesis of the siderophore pyoverdine. *Mol. Microbiol.* 45, 1673–1685.
- (38) Yeterian, E., Martin, L. W., Lamont, I. L., and Schalk, I. J. (2010a) An efflux pump is required for siderophore recycling by *Pseudomonas aeruginosa*. *Environ. Microbiol. Rep.* 2, 412–418.
- (39) Hannauer, M., Yeterian, E., Martin, L. W., Lamont, I. L., and Schalk, I. J. (2010) An efflux pump is involved in secretion of newly synthesized siderophore by *Pseudomonas aeruginosa*. *FEBS Lett.* 584, 4751–4755.
- (40) Leoni, L., Orsi, N., de Lorenzo, V., and Visca, P. (2002) Functional analysis of PvdS, an iron starvation sigma factor of *Pseudomonas aeruginosa*. *J. Bacteriol.* 182, 1481–1491.
- (41) Wilson, M. J., McMorran, B. J., and Lamont, I. L. (2001) Analysis of promoters recognized by PvdS, an extracytoplasmic

function sigma factor protein from *Pseudomonas aeruginosa*. *J. Bacteriol.* 18, 2151–2155.

(42) Poole, K., Neshat, S., Krebs, K., and Heinrichs, D. E. (1993) Cloning and nucleotide sequence analysis of the ferripyoverdine receptor gene *fpvA* of *Pseudomonas aeruginosa*. *J. Bacteriol.* 175, 4597–4604.

(43) Chen, Y., Jurkewitch, E., Bar-Ness, E., and Hadar, Y. (1994) Stability constants of pseudobactin complexes with transition metals. *Soil. Sci. Soc. Am. J.* 58, 390–396.

(44) Brayner, R., Ferrari-Iliou, R., Brivois, N., Djediat, S., Benedetti, M. F., and Fievet, F. (2006) Toxicological impact studies based on *Escherichia coli* bacteria in ultrafine ZnO nanoparticles colloidal medium. *NANO Lett.* 6, 866–870.

(45) Simon-Deckers, A., Loo, S., Mayne-L'Hermite, M., Herlin-Boime, N., Menguy, N., Reynaud, C., Gouget, B., and Carriere, M. (2009) Size-, composition- and shape-dependent toxicological impact of metal oxide nanoparticles and carbon nanotubes toward bacteria. *Environ. Sci. Technol.* 43, 8423–8429.

(46) Yang, W., Shen, C., Ji, Q., An, H., Wang, J., Liu, Q., and Zhang, Z. (2009) Food storage material silver nanoparticles interfere with DNA replication fidelity and bind with DNA. *Nanotechnology* 20, 08S102.

(47) Atha, D. H., Wang, H., Petersen, E. J., Cleveland, D., Holbrook, R. D., Jaruga, P., Dizdaroglu, M., Xing, B., and Nelson, B. C. (2012) Copper oxide nanoparticle mediated DNA damage in terrestrial plant models. *Environ. Sci. Technol.* 46, 1819–1827.

(48) Karlsson, H. L., Cronholm, P., Gustafsson, J., and Moller, L. (2008) Copper oxide nanoparticles are highly toxic: A comparison between metal oxide nanoparticles and carbon nanotubes. *Chem. Res. Toxicol.* 21, 1726–1732.

(49) Höfte, M., Dong, Q., Kourambas, S., Krishnapillai, V., Sherratt, D., and Mergeay, M. (1994) The *sss* gene product, which affects pyoverdine production in *Pseudomonas aeruginosa* 7NSK2, is a site-specific recombinase. *Mol. Microbiol.* 14, 1011–1020.

(50) Wu, B., Wang, Y., Lee, Y. H., Horst, A., Wang, Z. P., Chen, D. R., Sureshkumar, R., and Tang, Y. J. J. (2010) Comparative ecotoxicities of nano-ZnO particles under aquatic and aerosol exposure modes. *Environ. Sci. Technol.* 44, 1484–1489.

(51) Rossbach, S., Wilson, T. L., Kukuk, M. L., and Carty, H. A. (2000) Elevated zinc induces siderophore biosynthesis genes and a *zntA*-like gene in *Pseudomonas fluorescens*. *FEMS Microbiol. Lett.* 191, 61–70.

(52) Pabst, M. W., Anderson, A. J., Miller, C. D., Dimkpa, C., and McLean, J. E. (2010) Defining the surface adsorption and internalization of copper and cadmium in a soil bacterium, *Pseudomonas putida*. *Chemosphere* 81, 904–910.

(53) Miller, C. D., Pettee, B., Zhang, C., Pabst, M., McLean, J. E., and Anderson, A. J. (2009) Copper and cadmium: responses in *Pseudomonas putida* KT2440. *Lett. Appl. Microbiol.* 49, 775–783.

(54) Glover, R. D., Miller, J. M., and Hutchison, J. E. (2011) Generation of metal nanoparticles from silver and copper objects: nanoparticle dynamics on surfaces and potential sources of nanoparticles in the environment. *ACS Nano* 5, 8950–8957.